GDSPIKE: AN ACCURATE SPIKE ESTIMATION ALGORITHM FROM NOISY CALCIUM FLUORESCENCE SIGNALS

Jilt Sebastian[⋆]*, Mari Ganesh Kumar M*[⋆]*, Y. S. Sreekar*[⋆]*, Rajeev Vijay Rikhye*[†]
Mriganka Sur[†] *and Hema A. Murthy*[⋆]

[⋆]Department of Computer Science and Engineering, Indian Institute of Technology, Madras
[†]Department of Brain and Cognitive Sciences, Massachusetts Institute of Technology, Cambridge

ABSTRACT

Accurate estimation of spike train from calcium (Ca^{2+}) fluorescence signals is challenging owing to significant fluctuations of fluorescence level. This paper proposes a non-model-based approach for spike train inference using group delay (GD) analysis. It primarily exploits the property that change in Ca^{2+} fluorescence corresponding to a spike has a notable onset location followed by a decaying transient. The proposed algorithm, GDspike, is compared with state-of-the-art systems on five datasets. F-measure is best for GDspike (41%) followed by STM (40%), MLspike (39%), and Vogelstein (35%). While existing methods are inspired by the physiology of neuronal responses, the proposed approach is inspired by GD-based high-resolution processing of the Ca^{2+} fluorescence signal. GDspike is a fast and unsupervised algorithm. It is found to be unaffected when tested with five different GCaMP indicators and scanning rate varying from 15Hz to 60Hz.

Index Terms— spike train, Ca^{2+} fluorescence, group delay.

1. INTRODUCTION

Obtaining spiking inferences from neurons is extremely important for identifying the information processing task in local networks of neurons and for other higher level tasks in computational neuroscience. This is because neurons communicate primarily via action potentials. Accessing the activities of populations of neurons in *vivo* by means of Genetically-Encoded Calcium Indicator (GECI) proteins [1] or Oregon Green BAPTA (OGB) dye with two-photon imaging blurs individual spiking information. These Ca^{2+} fluorescence signals tend to be noisy with slow rise times and long decay tails, which carry very little information about the underlying spiking process. The actual neuronal action potentials need to be "filtered" from this signals for further processing.

However, this estimation is limited owing to the following reasons: First, background fluorescence varies with time and is indistinguishable from the fluorescence changes during spike occurrence. Second, the Ca^{2+} imaging and the fluorescence signals are contaminated by random noises of continuously varying energy levels. Third, the intracellular Ca^{2+} level transients have large time constants and several of such transients are non-linearly added causing difficulties in tracking the overlapping spikes [2].

Several methods proposed for inferring the spiking information can be categorized into model-based techniques and supervised methods. Various model-based techniques such as physiological models [3], template matching [4, 5], likelihood-based alignment, and approximate Bayesian inference based on deconvolution [6, 7] are limited by the noise statistics and model assumptions. Data-driven approaches including STM [8] and other simple learning techniques [9] need sufficient fluorescence traces with ground truth and often have a limited performance on unseen data. STM requires preprocessing of the Ca^{2+} fluorescence signals by linear regression fit and the spikes are modeled using a Poisson distribution [8, 10] which makes it again a model-dependent approach. The parameter λ is learned using a supervised model [11] and the evaluations consider the spiking probabilities, but not the "pulse-coded" spike train. Analyses inclusive of the spike train and its metrics are very important as they represent the information encoded by a neuron. In MLspike [3], the most probable spike train which maximizes the likelihood of the given Ca^{2+} fluorescence trace is computed. The algorithm is model-based and has high computational complexity owing to autocalibration of parameters.

This paper proposes a GD-based algorithm inspired from audio signal processing for obtaining the spiking information. The Ca^{2+} fluorescence signal is converted to a minimum phase sequence for which the group delay function is then computed. The high-resolution and the additive property of the minimum phase group delay function are exploited [12]. The performance of GDspike is compared with state-of-the-art systems considering both the "pulse-coded" spike train and the spiking information (from which the spike train is estimated) using F-measure, correlation, and Area Under the ROC (AUC). The proposed method outperforms all other methods for F-measure and performs comparable to

supervised-STM model for correlation and AUC.

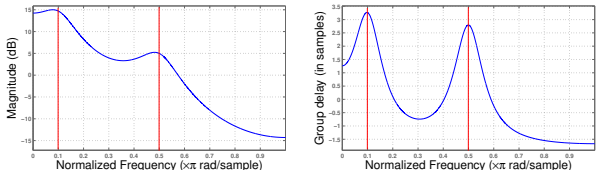

Fig. 1: Resolving power of the group delay function. *(left)* Magnitude spectrum and *(right)* Group delay spectrum for a two-pole minimum phase system.

2. PROPOSED WORK

2.1. Group Delay (GD) Function

The features used for the signal processing tasks are conventionally obtained either from the temporal or spectral domain. Spectral phase based features have recently been found to be effective in various tasks [12, 13, 14]. Although the information about a signal is present in both the magnitude and the phase spectra, the latter has not received much attention as Fourier analysis leads to the wrapped ($\pm\pi$) phase spectrum which makes it difficult to infer meaningful information. Among different phase domain alternatives, the group delay, and its derivatives are extensively used in audio signal processing tasks. The group delay function $\tau(\omega)$ of a discrete-time signal $x[n]$ is defined as:

$$\tau(\omega) = -\frac{d(\theta(\omega))}{d\omega} \tag{1}$$

where $\theta(\omega)$ is the continuous phase spectrum. Group delay could also be computed directly for minimum phase signals [15] as:

$$\tau(\omega) = \frac{X_R(\omega)Y_R(\omega) + X_I(\omega)Y_I(\omega)}{|X(\omega)|^2} \tag{2}$$

where $X(\omega)$ and $Y(\omega)$ denote the discrete-time Fourier transforms of $x[n]$ and $nx[n]$ respectively. R and I denote the real and the imaginary parts respectively.

2.2. Minimum Phase GD Processing

For a single resonator system, the ratio of the value of the peak in the magnitude spectrum to the value at a frequency that is n dB below the peak is always lower than that of the minimum phase group delay spectrum [12]. Using numerical analyses this higher-resolution property is extended for multiple resonators as well. For a cascade of resonators, the GD function exhibits high spectral resolution due to the additive property of poles in the phase domain. Figure 1 illustrates this phenomenon, where the example considered is a minimum phase system with two complex conjugate poles. It is evident that the peaks are better resolved in the GD domain compared to the magnitude spectrum.

For non-minimum phase signals, the zeros outside the unit circle in the Z-domain also appear as peaks in the GD domain in addition to the poles inside the unit circle. This limits the performance of group delay for signal processing applications since it is difficult to differentiate between the zeros outside and poles inside the unit circle. However, the minimum phase equivalent of a non-minimum phase signal can be obtained by taking the causal portion of the inverse Fourier transform of magnitude spectrum raised to a power of γ [16]. Exploiting this method, the minimum phase group delay has been extensively used for segmentation of speech into syllables [17, 16, 18] and for obtaining percussion stroke onsets [19].

2.3. GD for Spike Estimation

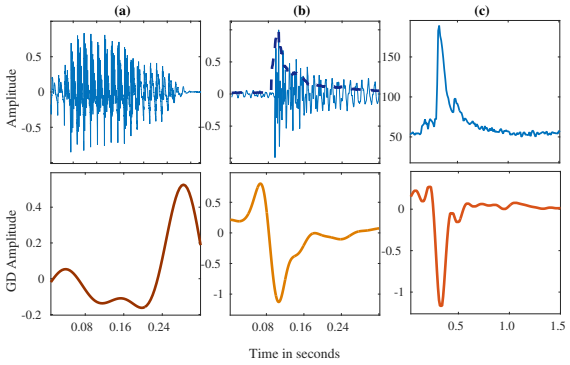

Fig. 2: Group delay domain representation for signal units comprising of an onset, an attack, and a decay. (a) A Hindi speech syllable (*"Va"*), (b) A percussive stroke in Mridangam (*"Tha"*), and (c) A Ca^{2+} fluorescence signal corresponding to an action potential. The bottom panel shows the corresponding minimum phase GD functions extracted from the top panel.

The fluorescence changes which corresponds to the neuronal firing is similar to that of syllables in speech and onsets in music signals (see Figure 2) though the durations are different. In speech signals, a syllable is the smallest meaningful production unit. Similarly, for a percussion instrument, a stroke is the fundamental production unit. In neuronal signals, an action potential is a fundamental unit which is observed as a fast rise and long decay tail in the Ca^{2+} signals (the latency is caused by the kinetics of calcium binding to the indicator). All the three signals exhibit an onset, an attack, and a decay. GD-based processing of such signals leads to signals that rise at the onset and taper exponentially away from the peak after the attack (In Figure 2, the bottom panel (a) shows inverse of GD, (b) and (c) shows GD). The time series is initially considered as the Fourier representation of a hypothetical minimum phase signal (Figure 3(a)). The GD of the hypothetical signal is computed using Equation 2 (Figure 3(b)). This signal

is then converted to a spike information via a simple triangle approximation step where peaks and valleys are replaced by zeros and midpoints between them are considered as new peaks (Figure 3(c)).

2.4. Algorithm

A brief overview of the algorithm is presented below:

Algorithm 1 GDspike Algorithm

Input: Fluorescence signal $C[n]$.
Output: Spike train $Sp[n]$.

1: Consider the fluorescence signal $C[n]$ as the magnitude spectrum of $h[n]$.
2: Compute $h[n] = F^{-1}(C[n] + C[-n])$.
3: Take causal portion of $h[n]$ limited to window scale factor ($\frac{length(h[n])}{WSF}$) to obtain minimum phase signal $h_1[n]$.
4: $GD[n]$ = Group delay of $h_1[n]$.
5: Find the zero crossing positions i in $GD^{'}[n]$ ($\forall i \in N$).
6: Compute $Sp[\frac{2i+1}{2}] = abs(GD[i] - GD[i+1])$ and $Sp[i] = 0, \forall i$.

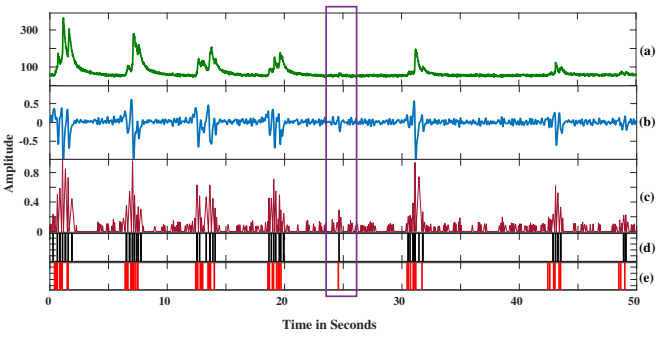

Fig. 3: GDspike Algorithm. (a) A segment of a fluorescence signal, (b) its minimum phase group delay representation, (c) the spike information, (d) predicted spike train, and (d) action potential ground truth.

Figure 3(a) shows a segment of normalized fluorescence signal taken from the 1^{st} neuron of GCaMP6f dataset [20]. It can be observed that most of the fluorescence changes are captured and the spike information has lower dynamic ranges which helps in thresholding to obtain the spike train (Figure 3(d)). The highlighted portion refers to a window with a hardly visible spike in the fluorescence segment that is detected by the proposed approach.

3. EXPERIMENTATION

3.1. Dataset

GDspike is evaluated the publicly available dataset provided by Svoboda lab, at Janelia Research Campus[1] ([21, 20, 22]). The dataset contains simultaneous loose-seal, cell-attached recordings (ground truth) and Ca^{2+} fluorescence imaging using GECI proteins with green and red fluorescence. These data are collected from the neurons of *in vivo* mice visual cortex. The ground truth recordings are obtained at a high sampling rate $\simeq 10kHz$ while the fluorescence imaging is recorded at a lower sampling rate, ranging from $15Hz$ to $100Hz$. A summary of the dataset is given in Table 1. The preparations are made using different scanning methods, leading to different sampling rates of the Ca^{2+} fluorescence imaging. Synthetic data is not considered for evaluations as it has been experimentally shown [8] that performances on actual and synthetic data vary significantly.

[1] http://crcns.org

Table 1: Dataset used for evaluation

Set	# cells	Indicator	Samp. Rate (in Hz)	Spikes	Ref.
1	9	GCaMP5k	50	2735	[21]
2	11	GCaMP6f	60	4536	[20]
3	9	GCaMP6s	60	2123	[20]
4	11	jRGECO1a	25	9080	[22]
5	10	jRCaMP1a	15	3624	[22]

3.2. Evaluation Metrics

Evaluation metrics considered in the literature focus either on the spike train [3, 7] or spike information [8], but not both. This work considers both of them and evaluates these algorithms on appropriate measures used in the literature. We are not considering the information gain [8] as a performance measure since it assumes a Poisson/non-linear model for the spike inference. All the measures are reported as an average across the datasets.

3.2.1. Area Under the Curve (AUC)

The AUC is measured as the area enclosed by the true positive rate (TPR) against the false positive rate (FPR) by varying the threshold of the spike information signal. It is the probability that an approach will rank a randomly chosen spike position higher than a randomly chosen position without any spike. AUC considers all the peaks above the threshold as spikes and is not sensitive to changes in the relative height at different temporal positions. AUC is suitable for algorithms for which a simple threshold is used to obtain the spike train from spike information, unlike MLspike [3].

3.2.2. Correlation

Correlation is a common evaluation measure used in the literature [8, 3] wherein the similarity of two signals are considered. Linear correlation coefficient is computed between every sample of the original and the estimated spike train. This measure alone is not enough for representing the performance of a spike train inference algorithm since it does not consider uncertainty of the predictions [8].

3.2.3. *F-measure*

F-measure is defined as the harmonic mean between sensitivity and precision. The spike predicted by a method is treated as *True Positive* if it is reported within a temporal bin of size $0.5s$ of the original spike train. The distance between the actual (ground truth) and estimated spikes are computed using a dynamic programming algorithm [23] which penalises the distance for spike deletions, insertions, and shifts.

3.3. Results and Analysis

Table 2: Performance of GDspike

Dataset	Recall	Prec.	F-measure	Corr.	AUC
GCaMP5k	0.57	0.68	0.43	0.070	0.84
GCaMP6s	0.82	0.60	0.49	0.022	0.86
GCaMP6f	0.79	0.68	0.55	0.035	0.80
jRGECO1a	0.52	0.38	0.31	0.034	0.71
jRCaMP1a	0.54	0.25	0.29	0.056	0.76

The results obtained by GDspike on each dataset (averaged across all the examples) is shown in Table 2. Observe that GDspike consistently performs well across all the preparations. Table 3 shows the average performance for three state-of-the-art algorithms namely, Vogelstein deconvolution algorithm, MLspike, and STM in comparison with GDspike. The algorithms used for comparison span over supervised [8], physiological model-based [3] and deconvolution [7] approaches. Other algorithms are not considered as it is shown in [8] that these algorithms outperform all the other approaches. The proposed approach significantly outperforms Vogelstein algorithm over all of the error measures and datasets. STM, being a supervised approach, performs well with the datasets which are similar to the training dataset. MLspike algorithm is computationally less efficient compared to Vogelstein and GDspike owing to the autocalibration time taken for the tuning of parameters. GDspike has best F-measure and comparable AUC with the STM approach across all the datasets.

Table 3: Average performance of different algorithms

Algo.	Recall	Prec.	F-measure	corr.	AUC
Vogelstein	0.398	0.705	0.345	0.036	0.64
STM	0.469	0.752	0.394	0.055	**0.80**
MLspike	0.826	0.508	0.407	0.067	0.58
GDspike	0.648	0.520	**0.413**	0.043	**0.79**

The results obtained by GDspike is analyzed on various counts. First, it is analyzed on the basis of the dataset. Figure 4 shows the performance measures in comparison with other algorithms in each of the preparations. The proposed algorithm outperforms STM and Vogelstein algorithms for most of the error measures on the most recent dataset (jRGECO1a and jRCaMP1a). STM, being a data-driven model, fails

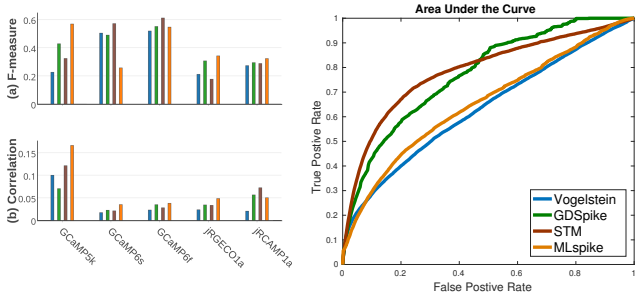

Fig. 4: Right panel shows the comparison of algorithms based on (a) F-measure and (b) Average correlation. Left panel is the ROC averaged across the datasets for different systems.

to achieve good evaluation measures for unseen data with a larger number of spikes and a lower scanning rate compared to other preparations. On the datasets GCaMP6f and GCaMP6s, GDspike outperforms Vogelstein and MLspike and has a comparable performance with that of STM in terms of F-measure. MLspike has the best F-measure for GCaMP5k dataset followed by GDspike.

Analysis based on error measures also favors the proposed approach. Figure 4(a) shows comparative evaluations of F-measure for each dataset. Observe that GDspike has consistent F-measure across the datasets with different scanning rates and indicator proteins, unlike STM and MLspike. GDspike gives the second best correlation for all the datasets except GCaMP5k (Figure 4(b)). The Right panel in Figure 4 shows the ROC[2] and it is inferred that GDspike outperforms all the unsupervised approaches and has comparable AUC values to that of the STM model.

4. CONCLUSION AND FUTURE WORK

A novel signal processing and non-model-based approach is proposed in this paper for extracting the spiking information from fluorescence signals. GDspike is able to resolve closely spaced tiny fluorescence peaks owing to the additive and high-resolution properties of the signal in the phase domain. It is evaluated using three metrics representing similarity to the actual spike train over five different datasets and is compared with three state-of-the-art algorithms. The proposed approach outperforms other approaches for F-measure and has comparable results to the supervised STM approach for AUC. One future direction would be to use the GD positions as a feature for training the supervised model to obtain the spike train.

[2]Source code, datasetwise ROC and examples at: `https://sites.google.com/site/groupdelayspike`

5. REFERENCES

[1] Tsai-Wen Chen et al., "Ultrasensitive fluorescent proteins for imaging neuronal activity," *Nature*, vol. 499, no. 7458, pp. 295–300, 2013.

[2] Jasper Akerboom et al., "Optimization of a gcamp calcium indicator for neural activity imaging," *The Journal of neuroscience*, vol. 32, no. 40, pp. 13819–13840, 2012.

[3] Thomas Deneux et al., "Accurate spike estimation from noisy calcium signals for ultrafast three-dimensional imaging of large neuronal populations in vivo," *Nature Communications*, vol. 7, no. July, pp. 12190, 2016.

[4] David S Greenberg, Arthur R Houweling, and Jason ND Kerr, "Population imaging of ongoing neuronal activity in the visual cortex of awake rats," *Nature neuroscience*, vol. 11, no. 7, pp. 749–751, 2008.

[5] Benjamin F Grewe et al., "High-speed in vivo calcium imaging reveals neuronal network activity with near-millisecond precision," *Nature methods*, vol. 7, no. 5, pp. 399–405, 2010.

[6] Eftychios A Pnevmatikakis, Josh Merel, Ari Pakman, and Liam Paninski, "Bayesian spike inference from calcium imaging data," in *2013 Asilomar Conference on Signals, Systems and Computers*. IEEE, 2013, pp. 349–353.

[7] Joshua T Vogelstein, Adam M Packer, Timothy A Machado, Tanya Sippy, Baktash Babadi, Rafael Yuste, and Liam Paninski, "Fast nonnegative deconvolution for spike train inference from population calcium imaging," *Journal of neurophysiology*, vol. 104, no. 6, pp. 3691–3704, 2010.

[8] Lucas Theis, Philipp Berens, Emmanouil Froudarakis, Jacob Reimer, Miroslav Román Rosón, Tom Baden, Thomas Euler, Andreas S Tolias, and Matthias Bethge, "Benchmarking Spike Rate Inference in Population Calcium Imaging.," *Neuron*, vol. 90, no. 3, pp. 471–82, 2016.

[9] Takuya Sasaki, Naoya Takahashi, Norio Matsuki, and Yuji Ikegaya, "Fast and accurate detection of action potentials from somatic calcium fluctuations," *Journal of neurophysiology*, vol. 100, no. 3, pp. 1668–1676, 2008.

[10] Robert E Kass and Valérie Ventura, "A spike-train probability model," *Neural computation*, vol. 13, no. 8, pp. 1713–1720, 2001.

[11] Lucas Theis, Andr Maia Chagas, Daniel Arnstein, Cornelius Schwarz, and Matthias Bethge, "Beyond GLMs: A Generative Mixture Modeling Approach to Neural System Identification," *PLoS Computational Biology*, vol. 9, no. 11, pp. e1003356, 2013.

[12] Jilt Sebastian, Manoj Kumar, and Hema A Murthy, "An analysis of the high resolution property of group delay function with applications to audio signal processing," *Speech Communication*, pp. 42–53, 2016.

[13] Zhizheng Wu, Chng Eng Siong, and Haizhou Li, "Detecting converted speech and natural speech for anti-spoofing attack in speaker recognition.," in *INTERSPEECH*, 2012, pp. 1700–1703.

[14] Pejman Mowlaee, Rahim Saeidi, and Yannis Stylianou, "Advances in phase-aware signal processing in speech communication," *Speech Communication*, vol. 81, pp. 1–29, 2016.

[15] Rajesh M Hegde, Hema Murthy, Venkata Ramana Rao Gadde, et al., "Significance of the modified group delay feature in speech recognition," *Audio, Speech, and Language Processing, IEEE Transactions on*, vol. 15, pp. 190–202, 2007.

[16] T Nagarajan, V Kamakshi Prasad, and Hema A Murthy, "Minimum phase signal derived from the root cepstrum," *IEE Electronics Letters*, vol. 39, pp. pp.941–942, June 2003.

[17] V K Prasad, T Nagarajan, and Hema A Murthy, "Automatic segmentation of continuous speech using minimum phase group delay functions," in *Speech Communications*, Apr. 2004, vol. 42, pp. 1883 – 1886.

[18] S Aswin Shanmugam and Hema A Murthy, "A hybrid approach to segmentation of speech using group delay processing and hmm based embedded reestimation," in *INTERSPEECH*, 2014.

[19] Manoj Kumar, Jilt Sebastian, and Hema A Murthy, "Musical onset detection on carnatic percussion instruments," in *Communications (NCC), 2015 Twenty First National Conference on*. IEEE, 2015, pp. 1–6.

[20] Tsai-Wen Chen et al., "Ultrasensitive fluorescent proteins for imaging neuronal activity.," *Nature*, vol. 499, no. 7458, pp. 295–300, 2013.

[21] J Akerboom, "Optimization of a GCaMP calcium indicator for neural activity imaging," *J. Neurosci.*, vol. 32, no. 40, pp. 13819–13840, 2012.

[22] Hod Dana et al., "Sensitive red protein calcium indicators for imaging neural activity.," *eLife*, vol. 5, pp. e12727, 2016.

[23] Jonathan D Victor and Keith P Purpura, "Nature and precision of temporal coding in visual cortex: a metric-space analysis," *Journal of neurophysiology*, vol. 76, no. 2, pp. 1310–1326, 1996.